2nd URSI AT-RASC, Gran Canaria, 28 May – 1 June 2018

Characterization of Indoor Visible Light Communication Channels and Design of a DCO-OFDM System

Dario Tagliaferri(1) and Carlo Capsoni(1,2)
(1) Dipartimento di Elettronica, Informazione e Bioingegneria, Politecnico di Milano, Italy
(2) Istituto di Elettronica e di Ingegneria dell'Informazione e delle Telecomunicazioni IEIIT, National Research

Abstract

This paper reports the implementation of a DCO-OFDM transceiver apt for indoor visible light communication scenarios, with particular emphasis on the sampling clock synchronization issue. Starting from the characterization of a typical indoor VLC channel in terms of impulse response and Signal-to-Interference-plus-Noise Ratio (SINR), the paper shows how a high-speed, robust communication can be provided by a DCO-OFDM system designed for working in realistic multipath channel scenarios and up to 300 ppm sampling clock offset.

1. Introduction

Visible light communication (VLC) systems make use of the available LED lamps to realize a high spatial density of high-speed optical links superposed to their natural illumination function. The envisaged application scenarios are mostly indoor, line-of-sight (LOS), such as offices, malls, etc., also E.M.I. free environments (hospitals, airplanes) [1]. VLC mainly differ from RF in the fact that the transmitted signal (as well as the optical channel) is purely real and non-negative. The usual transmission techniques must therefore be re-adapted to suit these conditions. The actual IEEE standard for VLC [2] employs only single carrier modulations (OOK, VPPM), which cannot exploit the full channel capacity. Moreover, although if actual LEDs have limited modulation bandwidth, the future development of wideband sources will lead to face multipath channels, against which single carrier modulations are not very robust. In addition, there is the need for flexible transmission techniques to serve multiple users requiring different service levels. In RF, all these issues are addressed with Orthogonal Frequency Division Multiplexing (OFDM), together with bit and power loading algorithms which can take advantage of the channel frequency variability and make use of high spectral efficiency modulations. One of the most widespread adaptations of OFDM to VLC is Direct Current Offset OFDM (DCO-OFDM), where the useful spectrum is reduced to half of the whole one to obtain a purely real signal (by forcing the Hermitian symmetry) and the 0-th subcarrier (DC) controls the illumination level, ensuring the non-negativity. Among the disadvantages of this approach, there is a high computational complexity and a strong sensitivity to time synchronization errors (since the carrier recovery is absent) [3]. In this work, we present first the analysis of a VLC channel inside a typical office room. Both the Channel Impulse Response (CIR) and the SINR are characterized, considering realistic transmitter-receiver configurations, so determining which values of signal bandwidth the channel is frequency-selective. Then we report the main features of the DCO-OFDM transceiver we developed, which can work in the previously mentioned scenarios up to 300 ppm of Sampling Clock Offset (SCO). The paper is organized as follows. Section 2 describe the analysis of VLC channel. Section 3 contains the description of the DCO-OFDM system. In Section 4, we present the results of some simulations proving the validity of our work and finally Section 5 concludes the paper.

2. Indoor VLC channel characterization

The VLC channel is mainly characterized by the channel impulse response between one or more sources and one receiver and by the SINR. While the first is a function of both the power budget and the geometry of the link, the second quantity is affected by many factors and its general expression is:

$$SINR = \frac{i_s^2}{i_{int}^2 + \sigma_{th}^2} \qquad (1)$$

where i_s is the electrical current produced by the useful signal (after the photodetector), i_{int} is the current produced by all the interfering lights (modulated) and σ_{th}^2 is the electronic noise variance, which is generated by the sum of all the non-modulated light sources (solar radiation and light fixtures) and the noise of the receiver itself (shot noises of the captured lights, dark current of the photodetector and front-end's noise). We made use of our ray tracing software (detailed in [4]) to simulate the light propagation and analyze both the CIR and the SINR

inside a typical office room, as the one depicted in Fig. 1. In this scenario, 8 non-directive (broadcast) light fixtures cooperate to serve a certain number of users (12), modeled as simple receiving units placed in random positions in space. The average distance of each receiver from the nearest source is 1.88 m. This scenario appears to be suitable for the application of a DCO-OFDM technique, where the whole spectrum (subcarriers) is dynamically subdivided and assigned to different users requesting different services, without generating mutual interference thanks to the orthogonality of the subcarriers. We take into considerations two practical cases: a (relatively) narrowband transmission with a signal bandwidth B of 10 MHz and a wideband one, where B is 100 MHz. Sources are assumed to emit a luminous power of 2000 lumens, distributed over a 3000 K white spectrum and to radiate on a 120° half power angle. Each receiver is equipped with 2 x Osram SFH2701 Si-PIN photodiodes, each one with 0.3 mm^2 area, 30 pA dark current, 60° field of view and 140 MHz bandwith, followed by a TransImpedance Amplifier (TIA) stage operated by a LTC6268-10 operational amplifier, whose overall input-referred current noise is optimized to be 0.26 $pA/\sqrt{Hz}$ for B = 10 MHz and 2.8 $pA/\sqrt{Hz}$ for B = 100 MHz. Table 1 reports the simulated SINR values at each receiver of Fig. 1. As previously mentioned, the assumption of perfect cooperation among the sources leads to a SINR determined only by the power budget and the amount of noise at the receiver, since the interference is absent. For B = 10 MHz, we have a maximum of 52.2 dB for Rx10 and a minimum of 48.6 dB for Rx9 (51.5 dB on average), while for B = 100 MHz the SINR decreases as the front-end's noise strongly increases. We observe a maximum of 28.2 dB and a minimum of 22.8 dB (26 dB on average). For widedand transmission, moreover, the optical channel is frequency-selective: Fig. 2 shows the CIR among all the sources (Tx1-Tx8) and Rx1 with its discrete time equivalent (with unit integral), whose taps are computed by integrating the CIR on time intervals equal to $T = 1/B$, for B = 100 MHz. In this case, in order to have a correct discrete-time modeling of the channel, at least 6 taps are necessary, since they contain 99.9% of the channel energy. By contrast, for B = 10 MHz, the channel is clearly impulsive.

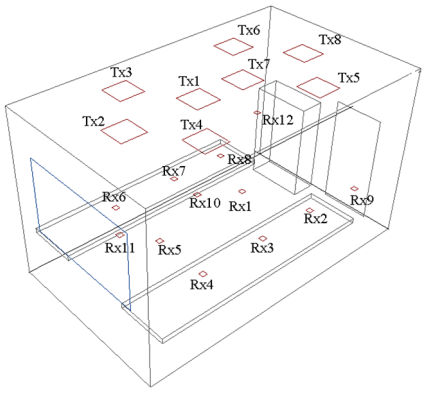

Figure 1. Typical office space as we modeled it in Autodesk 3DS Max.

Table 1. SINR values for each receiver of Fig.1.

Receivers	SINR [dB]	
	B = 10 MHz	B = 100 MHz
Rx1	51.5	27.5
Rx2	50.3	25.6
Rx3	50.6	26
Rx4	50	25.5
Rx5	50.8	25.7
Rx6	50.1	25.5
Rx7	50.6	26.1
Rx8	50.4	25.8
Rx9	48.6	22.8
Rx10	52.2	28.6
Rx11	50.5	26.5
Rx12	50.2	25.4

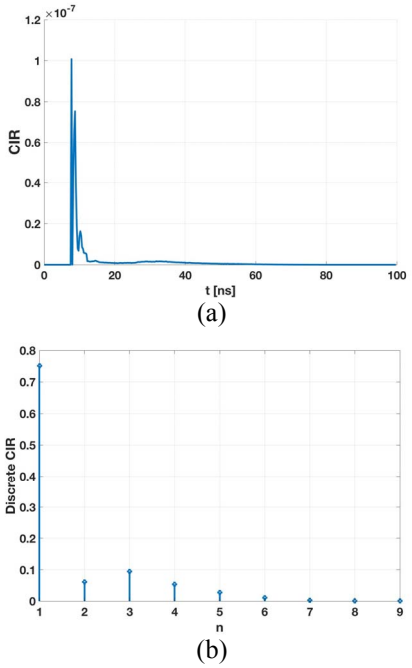

Figure 2. (a) Channel impulse response (CIR) from all the sources to receiver Rx1 of Fig. 1; (b) equivalent discrete channel response for B = 100 MHz, after removing the propagation delay.

3. DCO-OFDM System

3.1 DCO-OFDM Transmitter

The block diagram of the DCO-OFDM transmitter is very similar to the already existing ones, so it is not reported here. Let N be the FFT window size. Since the transmitted signal must be real, and this is accomplished by a Hermitian symmetry operation before the IFFT (discarding half of the spectrum), the maximum available number of subcarrier is $N/2 - 1$ (DC left for illumination). P subcarriers are eventually used as pilot tones. The transmitter therefore parallelizes the incoming

information symbols onto $N_u = N/2 - 1 - P$ channels and creates the frequency frame for the input of the IFFT. After that, a cyclic prefix of length $N_{cp} \geq L$ samples, where L is the maximum length of the channel, is affixed on each OFDM symbol to prevent inter-symbol interference (ISI). In our system, we decided to add also a cyclic suffix of length N_{cs} to be able to tolerate small timing synchronization errors. The transmission is divided in subsequent frames composed by N_s OFDM symbols preceded by a suitable preamble for the timing synchronization. The time signal after the framing operation (whose sampling time is $T = 1/B$) is oversampled by a factor F and passed through a pulse shaping filter (PSF) before going into the digital-to-analog converter (DAC) and then finally transmitted.

3.2 DCO-OFDM Receiver

The DCO-OFDM receiver must necessarily perform three operations before decoding the signal: a) synchronize the FFT window (symbol synchronization); b) synchronize the sampling clock; c) estimate and equalize the channel. In our work, which is based on the Ghimire [3] and Yang [5] ones, the time synchronization consists of two phases: a first, feed-forward acquisition of the FFT window position in time and a continuous, feedback tracking of the same to adjust for clock errors. The acquisition phase is further subdivided in two steps: a coarse estimation followed by a refined one based on the path time delay estimation [5]. For IM/DD OFDM the performance of the system is greatly affected by the time synchronization errors, and especially by the sampling clock frequency mismatches between transmitter and receiver (also called sampling clock offsets), which appear as time-varying time offsets causing inter-carrier interference (ICI) [3]. For single carrier modulations, the sampling clock recovery problem is approached with techniques that oversample (at least by a factor 4) and digitally interpolate the received signal, but these are not suitable for continuous-in-amplitude signals such as OFDM. In our work, as can be seen in Fig.4, the analog-to-digital converter (ADC) samples the received signal at double of the Nyquist frequency (2 samples per symbol) and keeps track of 3 versions of the signal (delayed one to the other by $T/2$): early (E), central (C) e late (L), necessary for the synchronization of the sampling clock.
The receiver is composed by 3 processing blocks (or branches) as in Fig. 4. The first one performs the coarse FFT window synchronization operating on the early, central and late branches by employing a Schmidl and Cox (S&C) preamble [6]. In practice, it finds the relative maximum (exceeding a fixed threshold) among the combination of the 3 S&C metrics on a time interval of N_{cp} . When the first block finds the maximum, it generates a trigger signal that enables the second block for the path time delay estimation, operating on the branch that presents the maximum metric. The path time delay, which is the integer part of the residual synchronization error (from the S&C estimation), is derived from the recursive channel estimation in frequency, obtained by averaging in

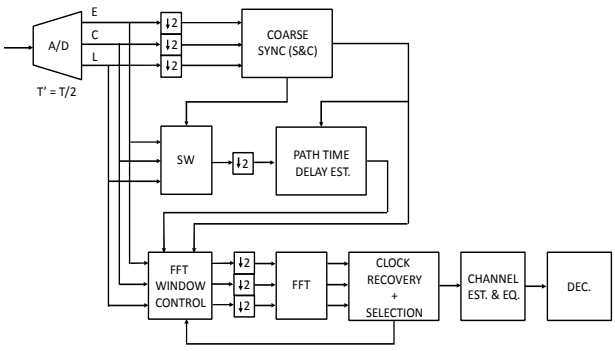

Figure 4. Block diagram of the DCO-OFDM receiver.

time on G pilot symbols that follow the S&C preamble [5]. Combined with the trigger signal, the path time delay adjusts an FFT window controller at the beginning of the third processing block. The latter uses the 3 available branches (E, C, L) to continuously compute the residual fractional delay (with granularity of $T/2$) to be put to the FFT window controller for compensate for the SCO. In practice, this block performs the cross-correlation between the 3 vectors of symbols received on the P pilot subcarriers (after the FFT) $\{Y_i^x\}_1^P$ and the vector of the pilot symbols $\{P_i\}_1^P$:

$$R^x = \sum_{i=1}^{P} Y_i^x \cdot (P_i)^* , \qquad x = E, C, L. \tag{2}$$

The receiver picks up the maximum of these 3 values, continuously adjusting (once every $T \cdot (N_{cp} + N + N_{cs})$ seconds) the FFT window in order to track the timing drift due to SCO. The branch with the maximum correlation is then used for least-squares estimating the channel and compensating for it before the final demodulation and decoding. This clock recovery technique shows to be sensitive and robust also in case of multipath channels, and requires a PSF at the transmitting side to be able to observe timing errors below T.

4. Simulations and Results

In order to show how the proposed system works, we considered the transmission between all the sources of Fig. 1 (Tx1-Tx8) to Rx1. We present the simulation, performed in MATLAB, of the uncoded bit error rate (BER) as function of the SCO in case of both narrowband (B = 10 MHz) and wideband communication (B = 100 MHz). We simulated the transmission of 10000 OFDM symbols for two FFT window sizes (N = 64 with P = 8 pilot tones and N = 128 with P = 16 pilot tones) and a SCO from 0 to 500 ppm. The goal is to show the combined impact of the FFT size N and the SCO on the performance of the system. In each simulation, the cyclic prefix has length N_{cp} = 10 samples and the cyclic suffix (for eventually absorbing small synchronization errors) has N_{cs} = 2 samples. For B = 10 MHz, we used the SINR value computed in Sect. 2 at the input of the ADC (51.5

dB), and we employed a 256-QAM as modulation on each data subcarrier, the latter chosen to exploit the channel capacity (8.4 bit/s/Hz in this case). The same approach applies to the wideband case (B = 100 MHz), where we used a 16-QAM modulation on a channel with capacity 4.56 bit/s/Hz (SINR = 27.5 dB). The coarse synchronization is carried out using a S&C preamble of length $N + N_{cp}$, and G = 5 pilot symbols are used for the path time delay estimation. The transmitter employs a digital raised cosine PSF obtained by oversampling by factor 4 the signal to be transmitted. Table 2 and Table 3 show the results.

As we can see, for both B = 10 MHz (impulsive channel) and B = 100 MHz (multipath channel), the system performance tends to worsen with increasing SCO and N (with the same SCO), as predicted by the theory [3]. This is due to the ICI effect which is a non-linearly increasing function of both SCO and N. For B = 10 MHz, the BER values are all below the FEC limit ($2 \cdot 10^{-3}$, [7]) for N = 64, while for N = 128 the maximum tolerable SCO is 400 ppm. For B = 100 MHz, however, the performance of the system in for small SCO values is dominated by the frequency-selective nature of the channel (BER due to channel fades) and the maximum allowable SCO (for which BER $\leq 2 \cdot 10^{-3}$) is 300 ppm (N = 128). There exists a trade-off to be considered when choosing the FFT size N: diminishing N leads both to a less complex hardware (whose computational complexity scales with $O(N \log_2 N)$) and to a more robust system against clock errors, but increasing N allows to obtain a higher resolution frequency estimation of the channel and to have more flexibility in the resource allocation process (for multiuser scenarios). For our purposes, N = 128 seems to represent a good compromise.

5. Conclusion

This paper reports the development of a DCO-OFDM system for VLC applications working in realistic link scenarios (simulated with our ray tracing software) and able to perform the complete physical synchronization task (symbol and clock recovery). The results show that, provided that the SCO is below 300 ppm, this system can guarantee BERs below the FEC limit using only two samples per symbol (allowing the use of moderate-to-low cost ADCs), even on typical multipath channels such as the ones occurring in offices.

Table 2. BER as function of both the SCO and the FFT window for B = 10 MHz (SINR = 51.5 dB, 256-QAM).

		N	
		64	128
SCO [ppm]	0	0	0
	100	$2.2 \cdot 10^{-6}$	$5.35 \cdot 10^{-5}$
	200	$6.7 \cdot 10^{-6}$	$1 \cdot 10^{-4}$
	300	$3.2 \cdot 10^{-4}$	$1.8 \cdot 10^{-3}$
	400	$2.9 \cdot 10^{-4}$	$2 \cdot 10^{-3}$
	500	$1.5 \cdot 10^{-3}$	$6 \cdot 10^{-3}$

Table 3. BER as function of both the SCO and the FFT window for B = 100 MHz (SINR = 27.5 dB, 16-QAM).

		N	
		64	128
SCO [ppm]	0	$8.4 \cdot 10^{-4}$	$5 \cdot 10^{-4}$
	100	$6.8 \cdot 10^{-4}$	$4.25 \cdot 10^{-4}$
	200	$6.7 \cdot 10^{-4}$	$4.77 \cdot 10^{-4}$
	300	$1.5 \cdot 10^{-3}$	$1.4 \cdot 10^{-3}$
	400	$1.88 \cdot 10^{-3}$	$2.2 \cdot 10^{-3}$
	500	$2.9 \cdot 10^{-3}$	$3.8 \cdot 10^{-3}$

6. References

1. T. Komine and M. Nakagawa, "Fundamental analysis for visible-light communication system using LED lights", *IEEE Transactions on Consumer Electronics*, **50**, 1, Feb 2004, pp. 100-107, doi:10.1109/TCE.2004.1277847

2. S. Rajagopal, R. D. Roberts and S. K. Lim, "IEEE 802.15.7 visible light communication: modulation schemes and dimming support", *IEEE Communications Magazine*, **50**, 3, March 2012, pp. 72-82, doi: 10.1109/MCOM.2012.6163585

3. B. Ghimire, I. Stefan, H. Elgala and H. Haas, "Time and frequency synchronisation in optical wireless OFDM networks" *2011 IEEE 22nd International Symposium on Personal, Indoor and Mobile Radio Communications*, Toronto, ON, 2011, pp. 819-823. doi:10.1109/PIMRC.2011.6140080

4. D. Tagliaferri and C. Capsoni, "SNIR predictions for on-aircraft VLC systems" *2016 International Conference on Broadband Communications for Next Generation Networks and Multimedia Applications (CoBCom)*, Graz, 2016, pp. 1-7, doi: 10.1109/COBCOM.2016.7593512

5. B. Yang, K. B. Letaief, R. S. Cheng and Z. Cao, "Timing recovery for OFDM transmission," in *IEEE Journal on Selected Areas in Communications*, **18**, 11, Nov. 2000, pp. 2278-2291, doi: 10.1109/49.895033

6. T. M. Schmidl and D. C. Cox, "Robust frequency and timing synchronization for OFDM" *IEEE Transactions on Communications*, vol. **45**, no. 12, Dec 1997, pp. 1613-1621, doi: 10.1109/26.650240

7. ITU-T Recommendation G.975.1 (02/2004)